Analysis of pixels in the region of interest using efficient segmentation methods and heat prediction for focused ultrasound interventions.

P. Revathy and V. Sadasivam.

***Abstract*— Lesion detection is a challenging task in the field of cancer imaging. In this research paper three efficient segmentation techniques are discussed to find the accurate Region of Interest (ROI). Image of liver cancer is taken for analysis. A new heat prediction method has been proposed and pixel wise heat prediction is done after applying the best method of segmentation. The heat prediction is done for High Intensity Focused Ultrasound (HIFU) interventions to treat cancer tissue by applying various ranges of heat intensities to ablate the tumor. The heat to be applied is compared for basic Pennes Bio-heat transfer equation (PBHTE) and the proposed heat prediction method.**

***Keywords*— Pennes bio-heat transfer equation, Threshold based segmentation, Active volume contour method, Level set segmentation.**

I. Introduction

HIGH intensity focused ultrasound (HIFU) is an imaging modality that provides cancer tissue removal by applying appropriate heat to the detected Region of Interest (ROI). Prediction of heat to be applied for HIFU treatment of abdominal organ like liver affected by tumor using Pennes Bio-heat heat prediction method considers the blood perfusion term as a constant. But the blood vessels passing through the liver carry away the heat to be applied to treat the affected area. Hence complete necrosis cannot be achieved. Also medical images are affected by intensity inhomogeneity, weak boundary, noise and the presence of similar objects close to each other. Segmentation of the tumor region from the liver is challenging.

A. Segmentation

Segmentation is the preprocessing step in any tumor detection process. In a heat treatment like HIFU the tumor region is segmented first for treatment planning. So proper segmentation of tumor region is important. A very basic segmentation method is intensity based segmentation which is otherwise called as threshold based segmentation. Thresholding type of segmentation can be done either locally or globally. In this research paper global type of segmentation is used for detection of tumor.

The tumor region is distinguished from the background by comparing with the threshold value chosen and then uses binary partition to segment the image. The threshold value is chosen such that the pixels that pass the threshold value are considered as the tumor object pixel and they are assigned with a binary value 1. Other pixels that do not pass the threshold value are assigned with a value 0 and they are the background pixels [1]. The most basic morphological operations used are dilation and erosion. The result of dilation is that, the output pixel is the maximum value of all the pixels in the input pixel's neighborhood. In a binary image, if any of the pixels is set to the value 1, the output pixel is set to 1, and for erosion, the value of the output pixel is the minimum value of all the pixels in the input pixel's neighborhood [2]. Canny edge detection method is a modification of Sobel method [3]. Canny edge detector implements Gaussian in its method to reduce the effect of noise during edge detection. Canny method provides sharpen edge detection compared to other edge detection methods [4]. Another popular method to segment medical images is the Chan Vese Active contour model otherwise called as Active contour model [5]. This method easily identifies the interior contours and also the objects whose boundaries are not defined by gradient. A classical snake model is an edge detector which detects the edged based on the gradient value of the image [6]. The initial contour detection is improved by Active contour model. This model works well for intensity inhomogeneity images [7]. Similar to active volume contour method, level set segmentation method is used successively for liver tumor segmentation with better preservation of details [8].

B. Similar Research

Various techniques for automatic segmentation of tumor in human liver are discussed by Vinita Dixit and Jyotika Pruthi [9]. When comparing the results of the proposed research with

P. Revathy is with PSN College of Engineering and technology, Tirunelveli, India. (+91 9962306042, kbrevathyseshu@gmail.com)

Dr. V. Sadasivam , is the Principal of PSN College of Engineering and Technology, Tirunelveli, India. (+91 9443286483, principal@psncet.ac.in)

relevant papers, the base temperature is taken as 37^0c by taking the standard value as absorption coefficient for human tissue. Also the temperature at the highly focused region is 65^0c in average
and in the off focus regions the temperature is 42^0c [10]. In the proposed research paper the base temperature of human tissue is taken as 37^0c for simulation. The absolute highest temperature measured for a single pixel was 97.8°C [11]. In reference paper [12] the author has discussed that good segmentation results were obtained by processing the intensity band of image.

C. Heat prediction by various thermal models for HIFU

After segmentation, pixel wise heat prediction is done for the segmented region. The heat transfer in the tissue and the temperature rise is based on Pennes Bio-Heat Transfer Equation (PBHTE) [13]. Thus the temperature and thermal dose to be applied to the region of interest are calculated. The physical phenomena of the living tissues are studied by the Bio-Heat Transfer Equations (BHTE). The tradition and the basic one is the Pennes bio-heat transfer equation. Other thermal models of bio-heat transfer are the extended and modified versions of the original work of Pennes. The Pennes bio-heat transfer equation for blood perfused tissues is written as,

$$(\rho C_\rho)_t \frac{\partial T_t}{\partial t} = \nabla.(K_t \nabla T_t) + q_p + q_m \quad (1)$$

Where q_p, q_m, ρ, $(C_\rho)_t$, T_t, K_t, t are the heat convention, metabolic heat transfer, tissue density, specific heat of tissue, temperature of tissue, thermal conductivity and time respectively. The advantage of PBHTE is that it predicts temperature fields and it is used in hyperthermia modeling. The limitation of PBHTE is that it does not consider the effect of the direction of blood flow. In PBHTE the blood perfusion term is proportional to temperature difference between two blood streams. This limitation is overcome by Wulff continuum model. In Wulff model the blood perfusion term is made proportional to the temperature difference between blood and tissue [14]. Wulff's equation is given as,

$$(\rho C_\rho)_t \frac{\partial T_t}{\partial t} = \nabla.(k_t \nabla T_t) - \rho_b V_h C_b \nabla T_b - \nabla H_b \nabla \phi \quad (2)$$

Where V_h, H_b, ρ_b, C_b and T_t are local mean blood velocity, specific enthalpy of blood, density of blood, specific heat of blood and tissue temperature respectively. The disadvantage of this method is that the local blood mass flux is hard to determine. The disadvantage of Pennes bio-heat model is that it neglects the effect of blood flow within the tissue. To overcome this, in Klinger continuum model the convective heat caused by blood flow in the tissue was considered [15]. Klinger continuum model is otherwise called as modified Penne's model equation and it is written as,

$$(\rho C_\rho)_t \frac{\partial T_t}{\partial t} + (\rho C)_b V_0 \nabla T_t = k \nabla^2 T_t + q_m \quad (3)$$

Where k_t, T_t, q_m and V_0 are the thermal conductivity, tissue temperature (convective heat caused by blood flow inside the tissue), metabolic heat transfer and the non-uniform velocity field respectively. Based on the discussion of the blood and tissue parameters [16], [17] and their values by comparing the Pennes BHTE, Wulff and Klinger, the proposed model of heat equation is formed.

II. PROPOSED HEAT EQUATION

To overcome the convective heat transfer problem and to predict the temperature in an efficient way, it is proposed to implement thermal dose and temperature prediction method based on varying blood perfusion.

A. New heat prediction equation by adding a parameter dynamic viscosity

The blood perfusion rate (ω_b) and the dynamic viscosity of blood (μ) values are added in the calculation of thermal dose for the proposed model. In the PBHTE the effect of blood flow within the tissue is neglected and in the proposed algorithm the perfusion rate and viscosity terms are taken into consideration [18]. Equation of the proposed algorithm is,

$$(\rho C)_t \frac{\partial T_t}{\partial t} = k_t \nabla^2 T_t - (\rho C)_b V_h \nabla T_t - (\rho C)_b \nabla T_t(\omega_b - \mu) + q_m \quad (4)$$

Where V_h= 10.5 m/s is the average blood velocity, ω_b = 0.5 kg/m^{3}s is the perfusion rate of the blood flow and μ= 0.004 kg/ms is the viscosity of blood.

III. RESULTS AND DISCUSSION

The input image of a tumorous liver is taken for analysis. The preprocessing stage before prediction of heat for tumor tissue is segmentation. A perfect segmentation technique is very important for finding the tumor region accurately. Complete ablation of tumor cells avoids recurrence of the cancer. In this research paper three methods to segment liver tumor targeted to support HIFU ablation are discussed. The results of various segmentation methods are analyzed.

A. Healthy and tumor pixels in the ROI

First the input image is segmented using threshold based segmentation. The result of segmentation by intensity based threshold segmentation is shown in Fig 1. The figure shows the

stages of segmentation done. Finally the ROI is obtained which is marked . There are totally 3078 pixel intensities in the segmented region by threshold method.

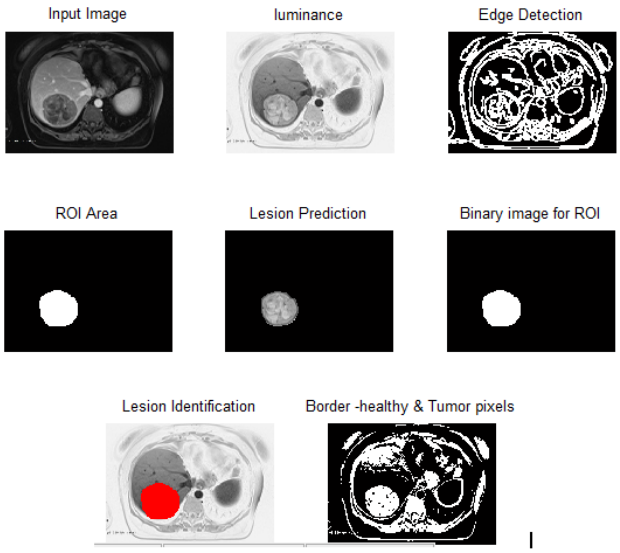

Fig 1. ROI identified by threshold based segmentation

Out of which 156 are healthy pixels and they lie in the intensity range 200 to 255. The remaining 2922 pixels are tumorous. Therefore 5.07% of pixels are healthy and 94.93% of pixels are tumorous. Next the input image is segmented using Active contour segmentation. The stages of the segmentation are shown in Fig 2.

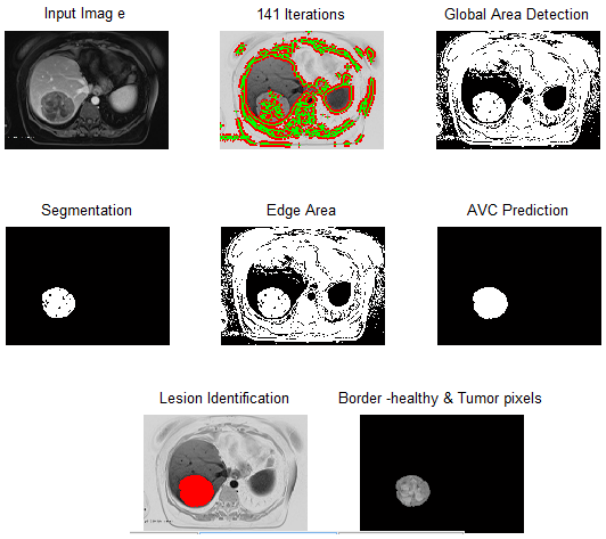

Fig 2. ROI identified by Active contour segmentation

There are totally 2725 pixels in the segmented region by threshold method. Out of which 92 are healthy pixels, which lie in the intensity range 200 to 255. The remaining 2633 pixels are tumorous. Therefore 3.38% of pixels are healthy and 96.62% of pixels are tumorous. Next the input image is segmented using Level set segmentation. The stages of the segmentation are shown in Fig 3.

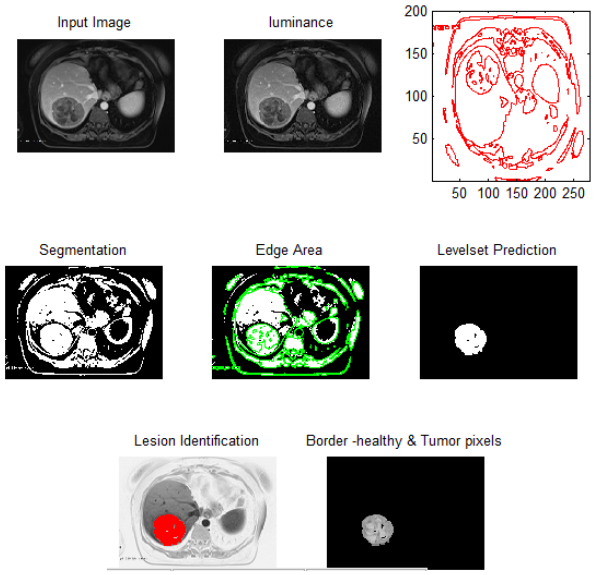

Fig 3. ROI identified by Active contour segmentation

The region segmented using Active contour method is small compared to the threshold method of segmentation. The number of heathy pixels identified in the tumor region is very low for the Active contour method and therefore less number of healthy pixels is affected by heat during treatment. The level set method has segmented the tumor region with 2842 pixels. Out of which 114 are healthy pixels and 2728 pixels are tumorous. Therefore 4.01% of the region in ROI is healthy and the remaining 95.99% are tumorous. Table I shows the size of the ROI, Number of tumor and healthy pixels in the ROI based on range of pixel intensities and the average intensity of pixels in the ROI.

Table I. Analysis of the Region of interest by various segmentation methods.

Segmentation method	Average intensity of pixels in the ROI	Size of ROI	Number of tumor and healthy pixels in the ROI based on range of pixel intensities		
			200 to 255	100 to 200	0 to 100
Threshold based segmentation	153.7297	3078	156	2578	344
Chan Vese Active contour Segmentation	156.8969	2725	92	2402	231
Level set segmentation	155.5609	2842	114	2486	242

From the above Table Active contour segmentation has segmented the tumor with less size of ROI and so very less number of healthy pixels are identified in the tumor region. But the other two methods have not segmented the tumor properly by not accounting the curves in the tumor region.

Table II. Percentage of tumor and healthy pixels in ROI

Segmentation method	Percentage of tumor and healthy pixels in the ROI based on range of pixel intensities		
	200 to 255	100 to 200	0 to 100
Threshold based segmentation	5.07	83.75	11.18
Chan Vese Active contour Segmentation	3.38	88.15	8.47
Level set segmentation	4.01	87.47	8.52

Table II shows the percentage of the healthy and tumor pixels in the total tumor region in three different intensity ranges. 200 to 255 which is the healthy portion, 100 to 200 which shows the region moderately affected by tumor and finally 0 to 100 shows the region highly affected by tumor. The number of healthy pixels in the tumor region for various segmentation methods is plotted in Fig 4.

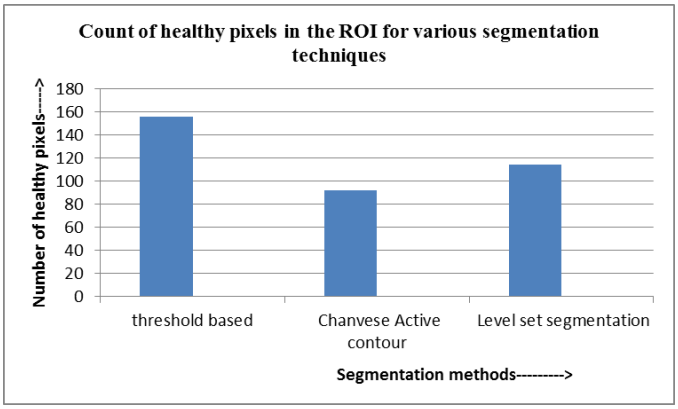

Fig 4. The number of healthy pixels in the ROI for various segmentation techniques.

The plot for the number of tumor pixels for various segmentation methods are shown in Fig 5.

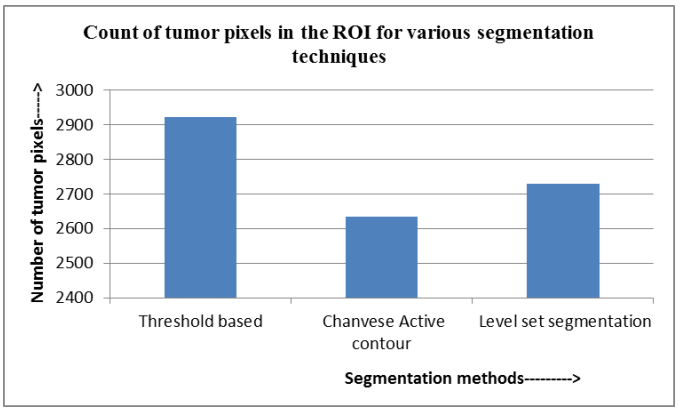

Fig 5. The number of tumor pixels in the ROI for various segmentation techniques.

B. Atlas based heat prediction

The result of heat predicted by PBHTE and Proposed heat prediction model are tabulated in Table III. An atlas is formed for all the pixel intensities from 0 to 255. 0 represents black which is highly tumorous and 255 represents white pixel ehich is healthy pixel. The heat predicted by PBHTE for the healthy pixel is 16.50^0c and that of the proposed model is 36.74^0c. The heat prediction for the healthy pixel intensity by proposed heat prediction model is more similar to the normal body heat which is 37^0c. From the Table III it is clear that the necessary heat for ablating the tumor tissue is predicted by the proposed heat prediction model. In the table below the predicted temperature values above 110^0c are not shown. The temperature within the tissue should be within the range 55^0c to 85^0c to destroy the tumor tissue completely [19]. As per the experimental results proven by Solovchuk [20] for temperature above 85°c, preboiling or cavitation occurs.

IV. CONCLUSION

Three different segmentation methods are analyzed to segment the tumor region in a MRI image of liver tumor. Chan Vese Active contour segmentation has segmented the tumor effectively as the number of healthy pixels in the tumor region is very low compared to the other two segmentation methods. Also from the atlas based temperature predicted by the proposed heat prediction method, the values of temperature predicted are more relevant to the similar research done in HIFU. This new temperature prediction method can be extended for 3D images and for tumor in other organs like brain and lungs.

Table III. The atlas of temperature values by PBHTE and Proposed heat prediction model.

Pixel Intensity	PBHTE	Proposed heat equation	Pixel Intensity	PBHTE	Proposed heat equation	Pixel Intensity	PBHTE	Proposed heat equation
91	107.1244	109.7473	146	33.2458	58.1987	201	21.1105	43.3831
92	103.0225	107.7819	147	32.8608	57.7776	202	20.9883	43.2152
93	99.2009	105.892	148	32.4859	57.3651	203	20.868	43.0496
94	95.634	104.0736	149	32.121	56.9609	204	20.7496	42.8862
95	92.299	102.3228	150	31.7656	56.5647	205	20.6331	42.725
96	89.1755	100.6363	151	31.4193	56.1763	206	20.5185	42.566
97	86.2455	99.0107	152	31.0819	55.7955	207	20.4056	42.4091
98	83.4926	97.4428	153	30.753	55.4221	208	20.2945	42.2543
99	80.9025	95.9299	154	30.4322	55.0558	209	20.1851	42.1014
100	78.462	94.4692	155	30.1194	54.6966	210	20.0773	41.9506
101	76.1594	93.0583	156	29.8142	54.3442	211	19.9712	41.8017
102	73.984	91.6947	157	29.5164	53.9983	212	19.8667	41.6548
103	71.9263	90.3762	158	29.2257	53.6589	213	19.7637	41.5097
104	69.9775	89.1008	159	28.9418	53.3258	214	19.6623	41.3664
105	68.1298	87.8663	160	28.6646	52.9988	215	19.5624	41.225
106	66.3759	86.6711	161	28.3938	52.6777	216	19.4639	41.0853
107	64.7093	85.5133	162	28.1292	52.3625	217	19.3669	40.9474
108	63.1241	84.3914	163	27.8706	52.0528	218	19.2712	40.8112
109	61.6146	83.3036	164	27.6178	51.7487	219	19.177	40.6767
110	60.176	82.2486	165	27.3707	51.4499	220	19.084	40.5438
111	58.8037	81.225	166	27.1289	51.1564	221	18.9924	40.4125
112	57.4934	80.2315	167	26.8925	50.868	222	18.9021	40.2828
113	56.2412	79.2668	168	26.6611	50.5845	223	18.813	40.1547
114	55.0435	78.3297	169	26.4347	50.3059	224	18.7252	40.0281
115	53.8972	77.4192	170	26.2131	50.032	225	18.6385	39.9031
116	52.799	76.5341	171	25.9962	49.7627	226	18.5531	39.7795
117	51.7462	75.6736	172	25.7837	49.4979	227	18.4688	39.6573
118	50.7362	74.8365	173	25.5757	49.2376	228	18.3856	39.5366
119	49.7666	74.022	174	25.3719	48.9815	229	18.3036	39.4173
120	48.835	73.2293	175	25.1722	48.7296	230	18.2226	39.2993
121	47.9394	72.4575	176	24.9765	48.4819	231	18.1427	39.1827
122	47.0779	71.7058	177	24.7847	48.2381	232	18.0639	39.0674
123	46.2487	70.9736	178	24.5967	47.9982	233	17.986	38.9535
124	45.45	70.2601	179	24.4123	47.7622	234	17.9092	38.8408
125	44.6802	69.5645	180	24.2316	47.5298	235	17.8334	38.7294
126	43.938	68.8864	181	24.0543	47.3012	236	17.7585	38.6192
127	43.2219	68.225	182	23.8803	47.0761	237	17.6846	38.5103
128	42.5306	67.5799	183	23.7097	46.8545	238	17.6116	38.4025
129	41.863	66.9503	184	23.5422	46.6363	239	17.5396	38.2959
130	41.2178	66.3358	185	23.3778	46.4214	240	17.4684	38.1905
131	40.594	65.7359	186	23.2165	46.2098	241	17.3981	38.0862
132	39.9907	65.1501	187	23.0581	46.0014	242	17.3286	37.983
133	39.4068	64.578	188	22.9026	45.7961	243	17.26	37.881
134	38.8415	64.0189	189	22.7498	45.5938	244	17.1923	37.78
135	38.294	63.4727	190	22.5998	45.3946	245	17.1253	37.6801
136	37.7634	62.9388	191	22.4524	45.1982	246	17.0592	37.5812
137	37.2491	62.4168	192	22.3077	45.0048	247	16.9938	37.4834
138	36.7502	61.9064	193	22.1654	44.8141	248	16.9292	37.3866
139	36.2663	61.4071	194	22.0256	44.6262	249	16.8654	37.2907
140	35.7965	60.9188	195	21.8881	44.441	250	16.8023	37.1959
141	35.3404	60.4409	196	21.753	44.2584	251	16.7399	37.102
142	34.8974	59.9733	197	21.6202	44.0784	252	16.6783	37.0091
143	34.4669	59.5155	198	21.4896	43.9009	253	16.6173	36.9171
144	34.0485	59.0673	199	21.3611	43.7259	254	16.5571	36.826
145	33.6416	58.6285	200	21.2348	43.5533	255	16.4975	36.7359

REFERENCES

[1] A. M. Khan, Ravi. S, "Image Segmentation methods : A comparative study," *Int.J. soft computing and engineering*, vol.3, Sep 2013, pp. 84-92.

[2] M. Ganesh, V. Palanisamy, "An Efficient Segmentation Technique for MRI Medical Images," *Int.J. Innovative Technology and Exploring Engineering*. vol.1, Oct 2012, pp. 70-73.

[3] Canny, J., "A Computational Approach to Edge Detection," *IEEE Trans. Pattern Anal Mach .Intell*, vol.8, Jun 1986, pp. 679-698.

[4] Nik Nur Zuliyana Mohd Rajdi, Lee Mee Yun, Heamn Noori Abduljabbar, Wan Mahani Hafizah, Joanne Soh Zi En, "Edge Detection and Diameter Measurement of Appendiceal Ultrasound Images for the assessment of Acute Appendicitis," *Advances in Environment Biotechnology and Biomedicine*, WSEAS Press, 330-335, (2012).

[5] E. Mendi and M. Milanova, " Image Segmentation with Active Contours Based on Selective Visual Attention," in Proc. 8th WSEAS Int.Conf. Signal Processing (SIP'09), Turkey 2009, pp.79-84.

[6] Tony F. Chan *a*nd Luminita A. Vese, "Active Contours Without Edges," *IEEE Transactions On Image Processing*, vol.10, Feb 2001, pp. 266-277.

[7] Rajalaxmi. S, Nirmala. S, "Automated Endo Fitting Curve for Initialization of Segmentation Based on Chan Vese Model," *J. Medical Imaging and Health Informatics*, vol.5, Sep 2015, pp. 572-580.

[8] Sørlie, Rune Petter. "Automatic segmentation of liver tumors from mri images." M.S. Thesis, Dept. Physics University of Oslo, 31ST AUGUST (2005).

[9] Vinita Dixit amd Jyotika Pruthi, "Review of Image Processing Techniques for Automatic Detection of Tumor in Human Liver," *International Journal of Computer science and Mobile computing*, vol.3, March 2014, pp. 371-378.

[10] Davies, Brian L., Sunita Chauhan, and Mike JS Lowe, "A robotic approach to HIFU based neurosurgery," Medical *Image Computing and Computer-Assisted Intervention, Springer*. vol. 1496 lecture notes in computer science, June 2006, pp. 386-396.

[11] Hansjörg Rempp, Rüdiger Hoffmann, Jörg Roland, Alexandra Buck , Antje Kickhefel and Claus D. Claussen, "Threshold-based prediction of the coagulation zone in sequential temperature mapping in MR-guided radio frequency ablation of liver tumors," *European Radiology*, vol.22, Nov 2011, pp. 1091-1100.

[12] Alsultanny, Yasa. "Color image segmentation to the RGB and HSI model based on region growing algorithm." *Proc. 4th WSEAS international conference on Computer engineering and applications*. World Scientific and Engineering Academy and Society (WSEAS), 2010.

[13] Sébastien Roujol, Baudouin Denis de Senneville, Silke Hey, Chrit Moonen and Mario Ries, "Robust Adaptive Extended Kalman Filtering for Real Time MR-Thermometry Guided HIFU Interventions," *IEEE Transactions On Medical Imaging*, vol. 31, March 2012, pp. 533-542.

[14] Wulff W, "The energy conservation equation for living tissue," *IEEE Transactions in Biomedical Engineering*, vol.6, 1974, pp. 494-495.

[15] H.G.Klinger, " Heat transfer in Perfused biological tissue -1," *General Theory in Bulletin of Mathematical Biology*, vol.36, 1974, pp. 403-415.

[16] Tzu-Ching Shih, Tzyy-Leng Horng, Huang-wen, Kuen Cheng, Tzung-chi Huang, " Numerical analysis of coupled effects of pulsatile blood flow and thermal relaxation time during thermal therapy," *Int.J.Heat and mass transfer*.vol.55, 2012, pp. 3763-3773.

[17] Shahnazari M, Aghanajafi C, Azimifar M and Jamali H, " Investigation of bioheat transfer equation of pennes via a new method based on wrm & homotopy perturbation," *Int.J. Research and Reviews in Applied Sciences*, vol.17, Dec.2013, pp. 306-314.

[18] P. Revathy, V. Sadasivam, "Analysis on the Healthy Pixels in the Region of Tumor and the Untreated Tumor Pixels in the Boundary During High Intensity Focused Ultrasound Interventions," Recent advances in computer science", in *Proc.*14th Int. conf. Applied computer and applied computational science, Malaysia, 2015, pp. 65-69.

[19] Solovchuk., Maxim A., San Chao Hwang., Hsu Chang., Marc Thiriet., Tony W.H Shew.: "Temperature elevation by HIFU in ex vivo porcine muscle: MRI measurement and simulation study." *Medical physics*, vol.41, April 2014, pp.1-13.

[20] Solovchuk, Maxim A,Tony W.H. Sheu, Marc Thiriet and Win-Li Lin, "On a computational study for investigating acoustic streaming and heating during focused ultrasound ablation of liver tumor," *Applied Thermal Engineering*.vol.56, July 2013, pp. 62-76.